BNL-102264-2014-TECH
RHIC/AP/159;BNL-102264-2013-IR

Nonlinear Diagnostics using an AC Dipole

S. Peggs

October 1998

Collider Accelerator Department
Brookhaven National Laboratory

U.S. Department of Energy
USDOE Office of Science (SC)

Notice: This technical note has been authored by employees of Brookhaven Science Associates, LLC under Contract No.DE-AC02-98CH10886 with the U.S. Department of Energy. The publisher by accepting the technical note for publication acknowledges that the United States Government retains a non-exclusive, paid-up, irrevocable, world-wide license to publish or reproduce the published form of this technical note, or allow others to do so, for United States Government purposes.

DISCLAIMER

This report was prepared as an account of work sponsored by an agency of the United States Government. Neither the United States Government nor any agency thereof, nor any of their employees, nor any of their contractors, subcontractors, or their employees, makes any warranty, express or implied, or assumes any legal liability or responsibility for the accuracy, completeness, or any third party's use or the results of such use of any information, apparatus, product, or process disclosed, or represents that its use would not infringe privately owned rights. Reference herein to any specific commercial product, process, or service by trade name, trademark, manufacturer, or otherwise, does not necessarily constitute or imply its endorsement, recommendation, or favoring by the United States Government or any agency thereof or its contractors or subcontractors. The views and opinions of authors expressed herein do not necessarily state or reflect those of the United States Government or any agency thereof.

RHIC/AP/159
October 29, 1998

Nonlinear diagnostics using an AC Dipole

S. Peggs, C. Tang

1 Introduction

Three goals are important when attempting to accurately diagnose nonlinear motion in a storage ring. First, it is necessary to move the beam out to the large amplitudes of interest – many times the natural beam size. Second, it is necessary to generate a strong and long lasting signal which is readily captured and analyzed. Third, it is highly desirable for the measurement technique to be non-destructive – especially, but not only, in hadron storage rings.

The common conventional technique is to use a strong single turn kick to move the beam out to large amplitudes, and then to record turn–by–turn signals on multiple beam position monitors [1–9]. In hadron and electron storage rings alike, this has the significant disadvantage that the finite tune spread causes the beam to filament in transverse phase space. The strong center of charge beam signal "decoheres" on a time scale that is often less than 100 turns. Filamentation also permanently destroys the emittance of the beam in a hadron ring, making it necessary to re-inject beam before another measurement can be made, or before the beams can be brought into collision. Hence, the "strong single turn kick" technique successfully achieves only one out of the three goals.

AC dipole techniques promise to achieve all three goals. Adiabatically excited AC dipoles coherently move the beam out to large amplitudes. Once there, the strong signals detected by the beam position monitors last arbitrarily long (in principle) – much longer than 100 turns – since the beam does not decohere. The beam returns to its original emittance if the AC dipoles are also turned off adiabatically, ready for another measurement, or ready for use in collisions.

The AGS has already had significant operating experience with a so called *RF dipole*, which has successfully enabled beams of polarized protons to accelerate through depolarizing resonances with minimal polarization loss [10, 11]. It accomplishes this by adiabatically exciting a coherent vertical betatron oscillation that is much larger than the size of the beam, at a drive tune that is close to the natural betatron tune. The AGS RF dipole is adiabatically turned

close to the natural betatron tune. The AGS RF dipole is adiabatically turned off when the resonance has been successfully negotiated, with no significant net emittance growth.

Learning from the AGS RF dipole experience, similar AC dipoles will be installed in RHIC – in the horizontal and vertical planes of both Blue and Yellow rings. This paper describes the beam dynamics theory of their anticipated use in nonlinear diagnostics measurements. The RHIC AC dipoles will also be used in other roles. They will be used to flip the spin of all the bunches in one ring during polarized proton operations. They will also be used at low excitation levels to measure linear optical functions by simultaneously recording turn–by–turn data in all beam position monitors [12].

This paper is organized as follows. First, the exact general solution to linear motion in the presence of an AC dipole is found, in a phasor description. Particular cases of interest are introduced. Second, an approximate Hamiltonian description of shear motion – linear motion plus amplitude detuning – is derived in the presence of an AC dipole. Third, nonlinear motion is discussed in a more general 2-D Hamiltonian formalism that does not include fully resonant motion.

Nonlinear diagnostics are most effectively performed using a *strong adiabatic drive* technique, as introduced above. The recorded time series is expected to be very long – perhaps 10,000 turns or more in practice. Fourier analysis of such a long time series generates easily resolved narrow peaks which stand high above the background noise level. This technique, the method of choice in RHIC, is discussed in detail.

In storage rings with the highest rigidities – much larger than those in RHIC – it might not be practical to build AC dipoles strong enough to move the beam out to large enough amplitudes. In this case a *hybrid* technique is viable, with both a strong one turn kick and a weak AC dipole simultaneously active. This technique is briefly discussed.

2 Linear motion with an AC dipole

With the AC dipole turned off, the one turn 1-D motion (horizontal, say) at a reference point is written

$$\begin{pmatrix} x \\ x' \end{pmatrix}_{t+1} = \begin{pmatrix} c & s \\ -s & c \end{pmatrix} \begin{pmatrix} x \\ x' \end{pmatrix}_t \tag{1}$$

where $c = \cos(2\pi Q_X)$, $s = \sin(2\pi Q_X)$, and Q_X is the betatron tune. The *normalized* coordinates x and x' both have the dimensions of length. They are related to the physical coordinates x_p and x'_p (which have the dimensions of length and angle) through

$$\begin{pmatrix} x \\ x' \end{pmatrix}_t = \begin{pmatrix} 1 & 0 \\ \alpha & \beta \end{pmatrix} \begin{pmatrix} x_p \\ x'_p \end{pmatrix}_t \tag{2}$$

where α and β are Twiss functions at the reference point. They are related to the normalized amplitude and phase a and ϕ through the equations

$$\begin{aligned} x &= a\,\sin(\phi) \\ x' &= a\,\cos(\phi) \end{aligned} \tag{3}$$

as sketched in Fig. 1.

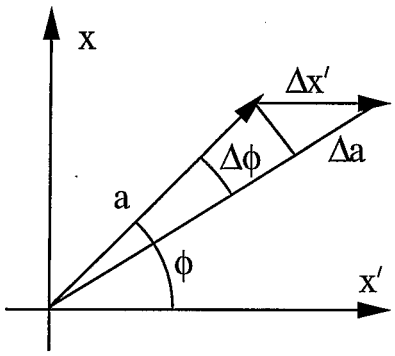

Figure 1: Normalized coordinate convention, and the effect of a dipole kick.

Horizontal motion is more concisely described using phasor notation to represent the normalized coordinates

$$z \equiv x' + i\,x \;=\; a\,e^{i\phi} \tag{4}$$

since then the one turn motion is just

$$z_{t+1} \;=\; R\,z_t \tag{5}$$

where $R = \exp(i\,2\pi Q_X)$. If the reference point is placed as shown in Fig. 2, then the normalized angle that the AC dipole adds at the beginning of turn t is represented as a *real* phasor increment

$$\begin{aligned} \Delta z_t \;=\; \Delta x' &= \delta\,\cos(2\pi Q_D t + \psi_0) \\ &= \frac{\delta}{2}\left[e^{i(2\pi Q_D t + \psi_0)} + e^{-i(2\pi Q_D t + \psi_0)}\right] \end{aligned} \tag{6}$$

where Q_D is the drive tune and ψ_0 is the initial phase. The normalized strength of the AC dipole is

$$\delta \;=\; \frac{BL}{(B\rho)}\,\beta_D \tag{7}$$

where BL is the integrated field amplitude, $(B\rho)$ is the rigidity, and β_D is the Twiss function at the dipole.

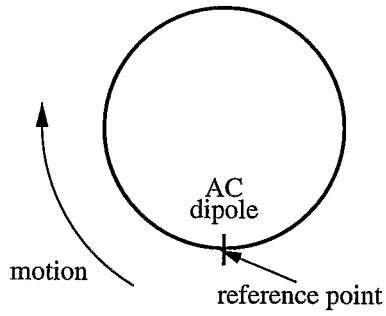

Figure 2: A simple storage ring with a reference point just before the AC dipole.

2.1 Exact solution of the equation of motion

If $z = z_0$ just before the first dipole kick, followed by kicks on turns $t = 0, 1, \ldots T-1$, then the net displacement phasor on turn T is

$$z_T = R^T z_0 + (R^T \Delta z_0 + R^{T-1} \Delta z_1 + \cdots + R^1 \Delta z_{T-1}) \tag{8}$$

which is expanded by substitution from Eqn. 6 to become

$$\begin{aligned} z_T &= R^T z_0 + R^T \frac{\delta e^{i\psi_0}}{2} [1 + R^{-1} d^1 + \cdots + R^{-(T-1)} d^{T-1}] \\ &\quad + R^T \frac{\delta e^{-i\psi_0}}{2} [1 + R^{-1} d^{-1} + \cdots + R^{-(T-1)} d^{-(T-1)}] \end{aligned} \tag{9}$$

where $d = e^{i2\pi Q_D}$. The two sums inside the square brackets of Eqn. 9 are of the general form

$$\Sigma = 1 + p + p^2 + ... + p^{T-1} \tag{10}$$

with

$$\begin{aligned} p &= e^{i2\pi Q_p} \\ &= e^{i2\pi(Q_D - Q_X)} \quad \text{or} \quad e^{-i2\pi(Q_D + Q_X)} \end{aligned} \tag{11}$$

This allows the use of the identity

$$\Sigma = \frac{p^T - 1}{p - 1} = \frac{e^{-i\pi Q_p}}{2 \sin(\pi Q_p)} (e^{i2\pi Q_p T} - 1) \tag{12}$$

to give the exact general solution for the linear motion

$$\begin{aligned} z_T &= R^T z_0 + R^T \frac{\delta}{4} \frac{e^{-i[\pi(Q_D - Q_X) - \psi_0]}}{\sin(\pi(Q_D - Q_X))} (e^{i2\pi(Q_D - Q_X)T} - 1) \\ &\quad - R^T \frac{\delta}{4} \frac{e^{i[\pi(Q_D + Q_X) - \psi_0]}}{\sin(\pi(Q_D + Q_X))} (e^{-i2\pi(Q_D + Q_X)T} - 1) \end{aligned}$$

This expression is simplified by introducing two complex AC dipole strengths

$$\begin{aligned} \delta_- &= \frac{\delta}{4} \frac{\exp(-i[\pi Q_- - \psi_0])}{\sin(\pi Q_-)} \\ \delta_+ &= \frac{\delta}{4} \frac{\exp(i[\pi Q_+ - \psi_0])}{\sin(\pi Q_+)} \end{aligned} \tag{13}$$

to hide the resonance denominators containing the two beating tunes

$$\begin{aligned} Q_- &= Q_D - Q_X \\ Q_+ &= Q_D + Q_X \end{aligned} \tag{14}$$

so that the exact general solution for linear motion becomes

$$z_T = R^T \left[z_0 - \delta_- \left(1 - e^{i2\pi Q_- T}\right) + \delta_+ \left(1 - e^{-i2\pi Q_+ T}\right)\right] \tag{15}$$

This becomes even more concise when it is written

$$\begin{aligned} z_T &= R^T \left[\widehat{z} + \delta_- e^{i2\pi Q_- T} - \delta_+ e^{-i2\pi Q_+ T} \right] \\ &= \widehat{z}\, e^{i2\pi Q_X T} + \delta_- e^{i2\pi Q_D T} - \delta_+ e^{-i2\pi Q_D T} \end{aligned} \tag{16}$$

where $\widehat{z} = z_0 - \delta_- + \delta_+$ is a constant given by the initial conditions. The behavior of this system becomes more clear when cases of particular interest are considered.

2.2 The oscillating closed orbit

In the absence of an AC dipole, the closed orbit is defined as that orbit which exactly repeats itself after one accelerator turn. This static definition is usefully extended to include an AC dipole by introducing an *oscillating closed orbit*, defined as that orbit which exactly repeats itself after one modulation period. The solution is trivially found by putting $\widehat{z} = 0$, so that

$$z_{CO} = \delta_- e^{i2\pi Q_D T} - \delta_+ e^{-i2\pi Q_D T} \tag{17}$$

since $Q_D T$ increases by 1 in one modulation period.

Thus the oscillating closed orbit follows an ellipse parameterized by the angle $2\pi Q_D T$ in normalized phase space. In general the ellipse is tilted, since δ_- and δ_+ are complex. The lengths of the semi-minor and semi-major axes are $||\delta_-| - |\delta_+||$ and $|\delta_-| + |\delta_+|$, so that the aspect ratio of the ellipse is

$$b_{CO} = \frac{|\delta_-| + |\delta_+|}{||\delta_-| - |\delta_+||} \tag{18}$$

In practice (see below) this ratio is often close to 1.

2.3 The rotating frame - dipole tune near the betatron tune

The response to an AC dipole is strongest when it is driven at a tune close to the fractional betatron tune. In this case $\sin(\pi Q_-) \approx 0$, so that $|\delta_-| \gg |\delta_+|$, in which case the equation of motion is

$$\begin{aligned} z_T &\approx R^T [\hat{z} + \delta_- e^{i2\pi Q_- T}] \\ &\approx \hat{z}\, e^{i2\pi Q_X T} + \delta_- e^{i2\pi Q_D T} \end{aligned} \tag{19}$$

This motion is the superposition of two rotating phasors of fixed length $|\hat{z}|$ and $|\delta_-|$, the first advancing by $2\pi Q_X$ per turn, and the second by $2\pi Q_D$ per turn.

It is sometimes more useful to picture the motion in a frame that rotates with the AC dipole drive, at $2\pi Q_D$ per accelerator turn. Motion in the rotating frame (denoted by over-bars) is simply

$$\overline{z}_T = \delta_- + \hat{z}\, e^{-i2\pi Q_- T} \tag{20}$$

so that a test particle slowly circulates the vector δ_-, with a displacement vector of constant length $|\hat{z}|$.

2.4 Adiabatic drive

What happens if the strength of the AC dipole δ_- is slowly ramped from zero to a constant value? Before the dipole is turned on $\hat{z}$ represents the initial conditions of the test particle. If it is a typical member of a bunch with an unnormalized root mean square emittance ϵ_u, then

$$|\hat{z}| \sim \sqrt{\beta \epsilon_u} \tag{21}$$

This length remains unchanged if the AC dipole is turned on slowly enough, as illustrated in Fig. 3, so that Eqn. 20 continues to apply

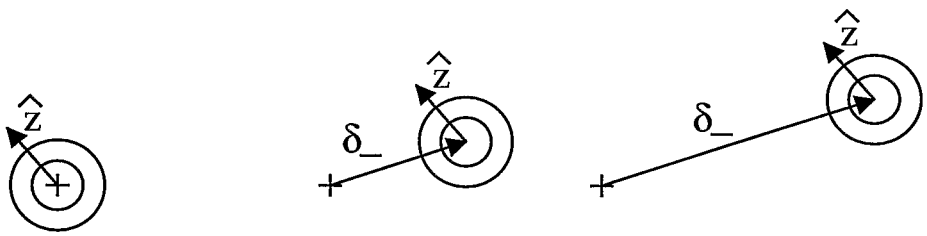

Figure 3: Sketches of the adiabatic excitation of an AC dipole, in the rotating frame. The circles represent the beam, which maintains a constant emittance as δ_- (the dipole excitation) increases.

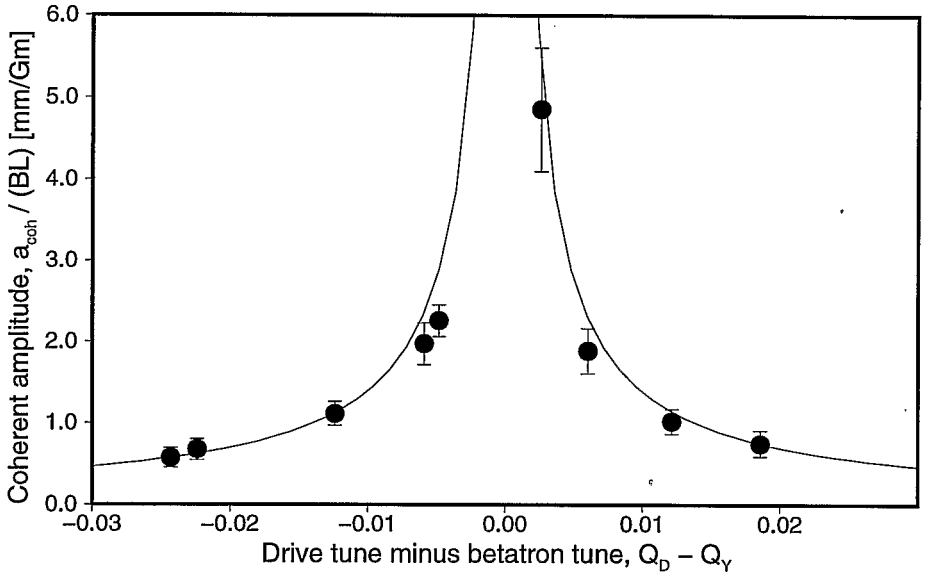

Figure 4: The amplitude of the center of charge of the coherent betatron response to the vertical AGS RF dipole, versus the difference between the dipole tune and the betatron tune.

$$\overline{z}_T \;=\; \delta_-(t) + \widehat{z}\, e^{-i2\pi Q_- T} \tag{22}$$

even when $\delta_-(t)$ is an explicit function of time.

When attention turns from the behavior of a single particle to the behavior of a bunch, a distribution of $\widehat{z}$ values must be taken into account. Particles with different values of $\widehat{z}$ simply circulate the same vector δ_-, advancing around the circles in Fig. 3 at a rate of $-2\pi Q_-$ radians per turn. Since the beam distribution is smoothly distributed around all phases $\widehat{\psi}$ of $\widehat{z}$, then

$$\begin{aligned} \langle \widehat{z} \rangle &= 0 \\ \langle \widehat{z}^2 \rangle &= 2\beta\epsilon_u \end{aligned} \tag{23}$$

where angle brackets $\langle\rangle$ represent a bunch average. The vector average of $\widehat{z}$ is zero, so the motion of the center of charge is just

$$\langle z_T \rangle \;=\; \delta_-\, e^{i2\pi Q_D T} \tag{24}$$

In other words, the response of a bunch to an adiabatically driven AC dipole is coherent, with an amplitude that is a constant of the motion

$$a_T \;=\; |\,\delta_-\,| \;=\; \frac{1}{4}\left|\frac{\delta}{\sin(\pi Q_-)}\right| \tag{25}$$

This confirms that maximum response is attained from an AC dipole of limited strength by setting Q_- as close as possible to zero.

2.5 AGS experience

Figure 4 shows measurements of the coherent betatron response of beam in the AGS as a function of $Q_- = Q_D - Q_Y$, the difference between the tune of the vertical dipole and the betatron tune [10]. The solid line is the prediction for this response given by Eqn. 25, in the absence of nonlinear detuning with betatron amplitude. Figure 5 shows beam profile measurements taken during an adiabatic excitation and de-excitation of the AGS RF dipole [10]. It shows no significant emittance growth, despite maximum amplitudes of 2 or 3 beam sigmas.

In general a bunch has a spread in Q_X values due to tune shift with momentum (chromaticity), and also due to nonlinear detuning. The spread in Q_X has the trivial affect of modifying the rate of advance around the δ_- vector, but it

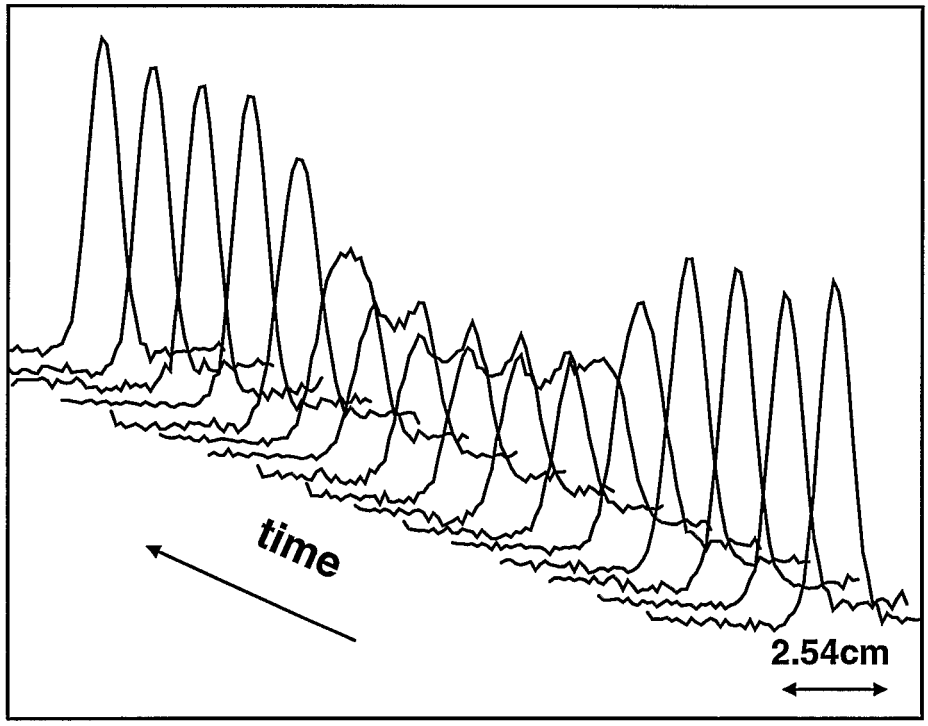

Figure 5: Ionization monitor beam profiles taken during adiabatic excitation and de-excitation of the AGS RF dipole, showing no net emittance growth.

also has the less trivial effect of modifying δ_-, which is a function of Q_- (see Eqn. 13). This is not a problem in practice if Q_D is sufficiently far outside the bunch tune spectrum.

2.6 Required AC dipole strength

Often it is useful to measure the size of the adiabatic amplitude in units of σ, the root mean square beam size. Putting all the factors together gives

$$\frac{a_T}{\sigma} = \frac{BL}{(B\rho)} \frac{1}{4\,|\sin(\pi Q_-)|} \sqrt{\frac{6\pi\beta_D\,\beta\gamma}{\epsilon}} \tag{26}$$

where ϵ is the normalized (6π) emittance. Note that $(B\rho)$ is proportional to the relativistic factor $\beta\gamma$, so that the amplitude measured in units of the beam size decreases with the square root of the rigidity, for a given ion species at a constant emittance.

This equation may be inverted to calculate the integrated field amplitude required in the AC dipole. For example, if an adiabatic amplitude of $a_T = 10\sigma$ is desired in RHIC at its maximum rigidity of $(B\rho) = 839.5$ [Tm], using an AC dipole with $|Q_-| = 0.01$ at a location where $\beta_D = 10$ [m], then

$$BL = 333.6\sqrt{\frac{\epsilon}{6\pi\,\beta\gamma}} \quad \text{[Tm]} \tag{27}$$

Gold ions have $\beta\gamma = 108.39$ at this rigidity. If they also have an emittance of $\epsilon = 40\pi \times 10^{-6}$ [m], then an integrated field amplitude of $BL = 0.0827$ [Tm] is required. Similarly, an integrated field amplitude of $BL = 0.0372$ [Tm] is required for protons with $\beta\gamma = 268.23$ and $\epsilon = 20\pi \times 10^{-6}$ [m].

2.7 Strong single turn kick with a weak AC dipole

Now consider what happens when conditions change very non-adiabatically. For example, suppose that the AC dipole is not strong enough to move the beam out to the large amplitudes of interest without the assistance of a strong single turn kick. In this scenario a kicker is fired during a period in which the AC dipole is maintained at a constant low level of excitation. Just after the transient

$$\begin{aligned} \langle\widehat{z}\rangle &= z_{kick} \gg \delta_- \\ \langle\widehat{z}^2\rangle &= z_{kick}^2 + 2\beta\epsilon_u \end{aligned} \tag{28}$$

as sketched in Fig. 6. The beam occupies only a narrow range of $\widehat{\psi}$ immediately after the kick, and rotates as a whole around the δ_- vector, just as in the adiabatic case. Because of the distribution in Q_X, the beam eventually filaments

to become uniformly spread in $\widehat{\psi}$, in a "hollow" beam that has a greatly increased emittance. Eventually

$$\begin{aligned} \langle \widehat{z} \rangle &= 0 \\ \epsilon_u(\text{final}) &= \epsilon_u(\text{initial}) + \frac{z_{kick}^2}{2\beta} \end{aligned} \tag{29}$$

The center of charge signal that is observed on beam position monitors decoheres with a characteristic time (in turns) of one over the tune spread. Typically this is of order 100 turns.

Even if the time that a coherent signal can be observed is short, the turn–by–turn normalized betatron amplitude is a physical observable of great practical interest. The amplitude of a single particle is independent of the frame in which it is measured

$$\begin{aligned} a_T &= |z_T| = |\overline{z}_T| \\ &\approx |\delta_- + \widehat{z}\, e^{-i2\pi Q_- T}| \end{aligned} \tag{30}$$

Assuming this equation to be exact, it is readily shown that in general

$$a_T^2 = |\widehat{z}|^2 + |\delta_-|^2 + 2|\widehat{z}||\delta_-| \cos(2\pi Q_- T + \psi_0 - \widehat{\psi} - \pi Q_-) \tag{31}$$

In the particular case at hand, taking $\widehat{z} = z_{kick}$ to represent a nominal particle at the center of the bunch, then the turn–by–turn amplitude observed on the beam position monitors is

$$a_T \approx |z_0| + |\delta_-| \cos(2\pi Q_- T + \psi_0 - \widehat{\psi} - \pi Q_-) \tag{32}$$

in the initial period before decoherence becomes significant.

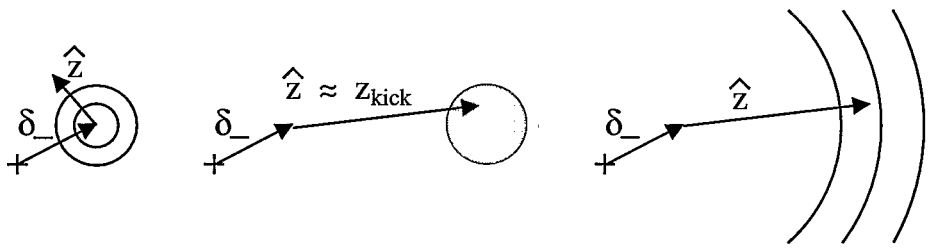

Figure 6: Sketches of the sudden excitation by a one turn kick, plus a constant AC dipole excitation, in the rotating frame. The beam has only a narrow range of $\widehat{\psi}$ immediately after the kick (middle). Eventually the beam filaments around the large circles, to acquire a much larger emittance (right).

A Discrete Fourier Transform of the turn–by–turn amplitude shows a peak at a tune $Q_{DFT} = Q_-$, in addition to any intrinsic peaks that are present due to accelerator nonlinearities. Intrinsic nonlinear peaks appear at aliased values given by

$$Q_{DFT} = |kQ_X + lQ_Y - m| \tag{33}$$

where it is always possible to find an integer m such that $0 < Q_{DFT} < 0.5$, for a given (k, l) pair of integers. The peak is wide when decoherence is strong, since the width is inversely proportional to the decoherence time. If the AC dipole peak at $Q_{DFT} = Q_-$ overlaps with an intrinsic peak, the two peaks interfere. Total destructive interference may be achieved by adjusting the tune, strength, and phase of the AC dipole. Thus, the single particle parameters which underly an intrinsic peak may be measured using an AC dipole, in a null measurement technique that works in the presence of strong decoherence. Despite its robustness, this is unfortunately a time consuming and destructive technique.

3 Shear motion with an AC dipole

The betatron amplitude and phase are modified when the beam receives a dipole kick. Assuming that $\Delta x'$ is small compared to a, the modifications are

$$\begin{aligned} \Delta a &= \Delta x' \cos(\phi) \\ \Delta \phi &= -\frac{\Delta x'}{a} \sin(\phi) \end{aligned} \tag{34}$$

as illustrated in Fig. 1. It is natural to convert to action-angle coordinates (J, ϕ) in a Hamiltonian description. If Δa is small the action kick is

$$\Delta J = \frac{a \Delta a}{\beta_D} \tag{35}$$

since the action is given by

$$J = \frac{1}{2} \frac{a^2}{\beta_D} \tag{36}$$

Note that the displacement x, the normalized angle x', the AC dipole strength δ, the action J, and the amplitude a all have the dimensions of length.

When the motion around the rest of the ring is included, the total one turn difference equation of motion becomes

$$\begin{aligned} \Delta J &= \frac{\delta}{\sqrt{\beta_D}} \sqrt{2J} \cos(2\pi Q_D t) \cos(\phi) \\ \Delta \phi &= -\frac{\delta}{\sqrt{\beta_D}} \frac{1}{\sqrt{2J}} \cos(2\pi Q_D t) \sin(\phi) + 2\pi(Q_{X0} + \alpha J) \end{aligned} \tag{37}$$

where the explicit time structure of the dipole kick is included from Eqn. 6, and where it is conveniently assumed that $\psi_0 = 0$. This motion includes a simple detuning term proportional to α, since (if $\delta = 0$)

$$Q_X(J) \equiv \frac{\langle \Delta\phi \rangle}{2\pi} = Q_{X0} + \alpha J \tag{38}$$

where angle brackets $\langle\rangle$ represent an average over many turns. Detuning that is linear in J is typical of the leading order dependence in real storage rings, usually due to the strong sextupoles that are used for chromaticity correction. Although these sextupoles do not cause any detuning to first order in their strength – in first order perturbation theory – they do to second order. The coefficient α is usually proportional to the square of the strength of the chromaticity correction sextupoles.

A *one turn discrete Hamiltonian* H_1 is now invoked to more concisely describe the motion from one turn to the next, through

$$\begin{pmatrix} \Delta J \\ \Delta\phi \end{pmatrix} = \begin{pmatrix} -\partial H_1/\partial\phi \\ \partial H_1/\partial J \end{pmatrix} \tag{39}$$

Since H_1 represents a *discrete* map, and not continuous motion, it is not (necessarily) even approximately a constant of the motion. In the case at hand the one turn Hamiltonian is

$$H_1 = 2\pi(Q_{X0}J + \frac{\alpha}{2}J^2) - \frac{\sqrt{2}\delta}{\sqrt{\beta_D}} J^{1/2} \cos(2\pi Q_D t) \sin(\phi) \tag{40}$$

Although it offers a concise description, this one turn Hamiltonian is limited in its usefulness by the fact that it is explicitly time dependent.

3.1 Transformation to the rotating frame

An approximately time independent Hamiltonian is found by applying the canonical transformation represented by the generating function

$$W(\overline{J}, \phi, t) = \overline{J}\phi - 2\pi Q_D \, t \, \overline{J} \tag{41}$$

The new action-angle coordinates and the new Hamiltonian (with over-bars) are related to the old ones through

$$\begin{aligned} J &\equiv \partial W/\partial\phi \\ \overline{\phi} &\equiv \partial W/\partial\overline{J} \\ \overline{H}_1 &\equiv H_1 + \partial W/\partial t \end{aligned} \tag{42}$$

In the particular case of the generating function in Eqn. 41, this leads to the transformed quantities

$$\begin{aligned} \overline{J} &= J \\ \overline{\phi} &= \phi - 2\pi Q_D\, t \\ \overline{H}_1 &= 2\pi(\frac{\alpha}{2}\overline{J}^2 - Q_-\overline{J}) - \frac{\sqrt{2}\delta}{\sqrt{\beta_D}}\overline{J}^{1/2}\cos(2\pi Q_D\, t)\ \sin(\overline{\phi} + 2\pi Q_D\, t) \end{aligned} \tag{43}$$

The net motion in one turn is now small if $Q_- = Q_D - Q_X \approx 0$ (and if δ is still assumed to be small).

Since the one turn motion is relatively small, it is legitimate to replace the trigonometric term in the expression for $\overline{H}_1$ by its average over many turns

$$\langle \cos(2\pi Q_D\, t)\ \sin(\overline{\phi} + 2\pi Q_D\, t)\rangle \ \approx\ \frac{1}{2}\sin(\overline{\phi}) \tag{44}$$

The one turn discrete Hamiltonian finally become time independent

$$\overline{H}_1(\overline{J},\overline{\phi}) \ = \ 2\pi(\frac{\alpha}{2}\overline{J}^2 - Q_-\overline{J}) \ - \ \frac{\delta}{\sqrt{2\beta_D}}\overline{J}^{1/2}\ \sin(\overline{\phi}) \tag{45}$$

and is a good approximation to a constant of the motion. It represents motion in a frame which rotates with the AC dipole kick, at an angular speed of $2\pi Q_D$ per turn relative to the physical (x, x') plane.

3.2 Fixed points of the motion

A fixed point $(\overline{J}_{FP}, \overline{\phi}_{FP})$ of this motion satisfies the equations

$$\begin{pmatrix} \Delta\overline{J} \\ \Delta\overline{\phi} \end{pmatrix} = \begin{pmatrix} -\partial\overline{H}_1/\partial\overline{\phi} \\ \partial\overline{H}_1/\partial\overline{J} \end{pmatrix} = \begin{pmatrix} 0 \\ 0 \end{pmatrix} \tag{46}$$

The first of these equations is

$$\frac{\delta}{\sqrt{2\beta_D}}\overline{J}_{FP}^{1/2}\ \cos(\overline{\phi}_{FP}) \ = \ 0 \tag{47}$$

with the simple solution

$$\overline{\phi}_{FP} \ = \ \pm\frac{\pi}{2} \tag{48}$$

After substitution using Eqn. 48, the second fixed point equation becomes

$$2\pi(\alpha\overline{J}_{FP} - Q_-) \ \mp \ \frac{\delta}{2\sqrt{2\beta_D}}\frac{1}{\overline{J}_{FP}^{1/2}} \ = \ 0 \tag{49}$$

where the $\mp$ sign corresponds to the $\pm$ sign in Eqn. 48.

In general when detuning is present, $\alpha \neq 0$, Eqn. 49 is cubic in $\overline{J}_{FP}^{1/2}$, with one or three roots. Depending on the strength of the detuning, there is either

one stable fixed point or one unstable and two stable fixed points [10, 11]. In the simplest case when detuning is absent, $\alpha = 0$, the action of the fixed point is given by

$$\overline{J}_{FP}^{1/2} = \frac{1}{4\pi\sqrt{2\beta_D}} \left| \frac{\delta}{Q_D - Q_{X0}} \right| \tag{50}$$

and the betatron amplitude is

$$a_{FP} = \frac{1}{4\pi} \left| \frac{\delta}{Q_D - Q_{X0}} \right| \tag{51}$$

in agreement with Eqn. 25 in the limit when $Q_D - Q_{X0}$ is small. Phasor and Hamiltonian descriptions give equivalent results!

3.3 A simple numerical example - part 1

Figure 7 illustrates the appearance of a fixed point in (a, ϕ) phase space, using a very simple numerical model in which detuning is driven by three octupoles which are spaced 60 degrees apart in phase [7, 13]. This spacing minimizes their resonance driving effect, resulting in very smooth shear motion when the AC dipole is turned off. A fixed point appears when the AC dipole is turned on, with its center at about $a \approx 0.66$ (arbitrary units). The dipole tune $Q_D = 59/101 \approx 0.584$, so the natural Poincare surface of section in the bottom plot is one modulation period of 101 turns. This tune was chosen to be out of the natural tune range, from approximately 0.591 to 0.609, which straddles the $Q_x = 3/5$ resonance. The stage is set for a single decapole to be added to the numerical model, to drive this resonance and to create ripples in the fabric of the shear motion.

Motion near a nonlinear fixed point is often characterized by the *island tune* Q_I of small oscillations around the fixed point. This quantity is usually calculated by expanding the Hamiltonian around the fixed point, and linearizing the motion to appear as simple harmonic motion. This procedure is not necessary in the linear case of the AC dipole with no detuning, since the phasor framework provides an exact description. Equation 20 shows that the island tune is just

$$Q_I = Q_{X0} - Q_D = -Q_- \tag{52}$$

However, the phasor description is incapable of handling even the mildest nonlinearity, such as shear motion. Although the Hamiltonian approach is only exact in trivial cases, it is unrivaled when used to describe general nonlinear motion, as below.

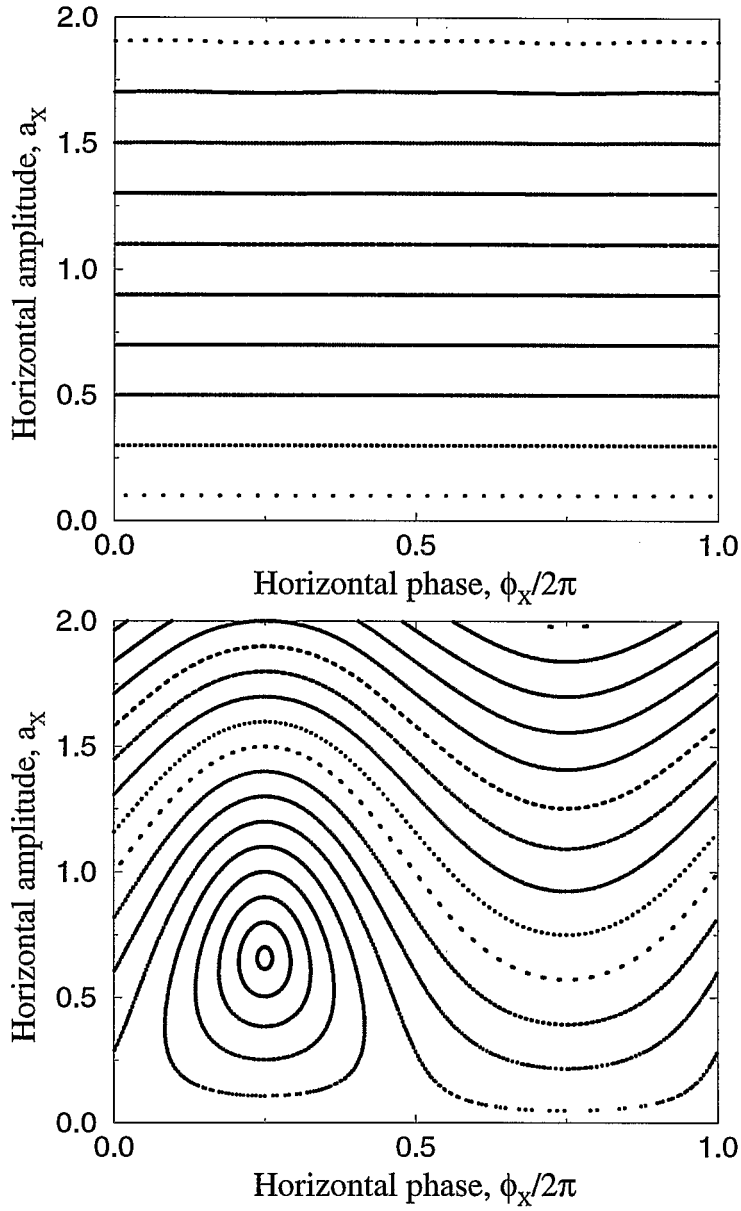

Figure 7: Fixed point due to an AC dipole in the presence of detuning. The TOP figure shows smooth shear motion with the AC dipole off, as the free tune shifts from 0.591 at zero amplitude to 0.609 at the maximum amplitude. The BOTTOM figure shows the fixed point generated by turning the AC dipole on, at a tune of $Q_D = 59/101 \approx 0.584$.

4 Nonlinear motion in 2-D

Nonlinear dynamics experiments often record the turn–by–turn time series $(x_1, x_2, y_1, y_2)_t$ observed at 2 horizontal and 2 vertical planes of neighboring beam position monitors. In a Hamiltonian framework it is natural to discuss the action-angle time series $(J_x, \phi_x, J_z, \phi_z)_t$ at a single reference point in the ring. In practice it is usually easy to construct the action-angle time series from the time series data, by empirically adjusting the ratio of the β functions at the two beam position monitors in each plane, and by adjusting the phase advance between them [1, 3, 6, 7]. This calibration adjustment compensates for inevitable linear optics errors. It also corrects for the linear elliptical motion of the oscillating closed orbit, when coherent motion driven by an AC dipole is being observed.

4.1 Distortion surfaces

In the general case of 2-D nonlinear motion the form of the one turn discrete Hamiltonian is

$$\begin{aligned} H_1 &= 2\pi Q_{X0} J_x + 2\pi Q_{Y0} J_y \\ &+ \sum_{ijkl} V_{ijkl} J_x^{i/2} J_y^{j/2} \sin(k\phi_x + l\phi_y + \phi_{ijkl}) \end{aligned} \tag{53}$$

where the appropriate set of indices $(ijkl)$ depends on the dominant nonlinearities [2]. For example, if sextupoles are being considered to first order then

$$(ijkl) = (3030, 3010, 1210, 1212, 121{-}2) \tag{54}$$

Only in the simplest of models can V_{ijkl} and ϕ_{ijkl} be predicted analytically – for a realistic storage ring a detailed numerical simulation is required.

One way to represent the motion is through the *distortion surfaces* $J_x(\phi_x, \phi_y)$ and $J_y(\phi_x, \phi_y)$ that the motion follows in (ϕ_x, ϕ_y) space. Good approximations to these surfaces are found by substituting first order solutions for $\phi_x(t)$ and $\phi_y(t)$ into the equations

$$\begin{aligned} J_x(\phi_x(t+1), \phi_y(t+1)) - J_x(\phi_x(t), \phi_y(t)) &= -\frac{\partial H_1}{\partial \phi_x} \\ J_y(\phi_x(t+1), \phi_y(t+1)) - J_y(\phi_x(t), \phi_y(t)) &= -\frac{\partial H_1}{\partial \phi_y} \end{aligned} \tag{55}$$

Natural first order solutions to the motion are

$$\begin{aligned} \phi_x(t) &= \phi_{x0} + 2\pi Q_X t \\ \phi_y(t) &= \phi_{y0} + 2\pi Q_Y t \\ J_x(t) &= J_{x0} \\ J_y(t) &= J_{y0} \end{aligned} \tag{56}$$

When Eqn. 56 is substituted into Eqn. 55, the horizontal distortion surface becomes

$$\begin{aligned} J_x(\phi_x,\phi_y) &= J_{x0} - \sum_{ijkl} \frac{k\, V_{ijkl}}{2\sin[\pi Q_{kl}]} J_{x0}^{i/2} J_{y0}^{j/2} \\ &\times \quad \sin(k\phi_x + l\phi_y + \phi_{ijkl} - \pi Q_{kl}) \end{aligned} \tag{57}$$

A similar expression for the vertical surface $J_y(\phi_x,\phi_y)$ is obtained by replacing $k\,V_{ijkl}$ with $l\,V_{ijkl}$. A single term in the sum dominates the distortions if the harmonic tune

$$Q_{kl} \equiv kQ_X + lQ_Y \tag{58}$$

approaches an integer for some (k,l) pair – if the lattice is close to a nonlinear resonance.

4.2 A simple numerical example - part 2

What do Q_X, Q_Y, J_{x0} and J_{y0} represent in Eqns. 56 and 57? In the simplest analysis $Q_X = Q_{X0}$, the tune of small amplitude motion. Alternatively, detuning is approximately taken into account by using

$$Q_X = Q_{X0} + \frac{1}{4\pi} \sum_{ij} i\, V_{ij00} J_{x0}^{(i-2)/2} J_{y0}^{j/2} \sin(\phi_{ij00}) \tag{59}$$

although this becomes incorrect in the vicinity of resonances. Similarly, J_{x0} and J_{y0} may be taken to represent average actions in the case of single particle motion.

This is appropriate for the top set of horizontal distortion surfaces shown in Fig. 8, which illustrates what happens in 1-D when a single decapole is added to the shear motion previously shown at the top of Fig. 7. A string of resonance islands appears at an amplitude of $a_{RES} \approx 1.4$, while the nearby surfaces suffer a fifth harmonic distortion. The V_{5050} term dominates [2].

It is of great interest to consider coherent motion driven by AC dipoles. In this case

$$\begin{aligned} Q_X &= Q_{DX} \\ Q_Y &= Q_{DY} \\ J_{x0} &= J_{xFP} \\ J_{y0} &= J_{yFP} \end{aligned} \tag{60}$$

so that Q_X, Q_Y, J_{x0} and J_{y0} represent the tunes and actions of simultaneous horizontal and vertical fixed points. Equation 57 then becomes the nonlinear analog of the linear Eqn. 17 for the oscillating closed orbit. It describes, for example, the distortion surface followed in the turn–by–turn motion of the fixed

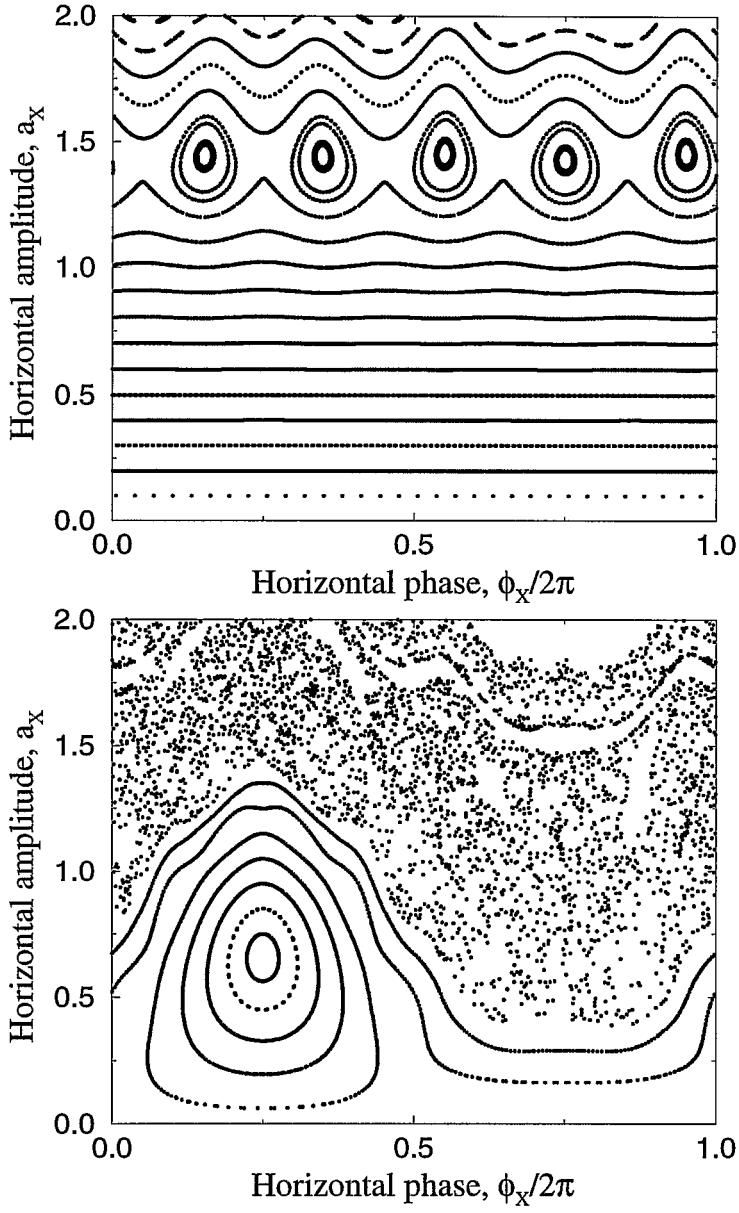

Figure 8: Motion near a decapole driven resonance, with an AC dipole and detuning. The TOP figure shows resonances islands with $Q_x = 3/5$ at $a_{RES} \approx 1.4$, when the AC dipole is off. The BOTTOM figure shows large scale stability around the fixed point when the AC dipole is turned on.

point shown in the bottom phase space portrait of Fig. 8. This corresponds to the bottom of Fig. 7, but now with the decapole turned on as well as the AC dipole. Here again the Poincare surface of section is one modulation period of 101 turns. The phase space regions where the resonance islands used to be are now chaotic (but stable). Nonetheless, there is still large scale stability around the fixed point where an adiabatically driven coherent beam would reside.

4.3 Diagnosis of action time series

The action time series $J_x(t)$ and $J_y(t)$ are directly accessible through beam position monitor turn–by–turn measurements. Approximate solutions for the time series are found by substituting $\phi_x(t)$ and $\phi_y(t)$ from Eqn. 56 into the the right hand side of Eqn. 57, to give

$$J_x(t) \;=\; J_{x0} - \sum_{ijkl} \frac{k\, V_{ijkl}}{2\sin[\pi Q_{kl}]}\; J_{x0}^{i/2} J_{y0}^{j/2}\; \sin(2\pi Q_{kl}\, t + \phi_{0ijkl}) \qquad (61)$$

where a similar expression for $J_y(t)$ is again obtained by replacing $k\, V_{ijkl}$ with $l\, V_{ijkl}$. The horizontal time series is conveniently rewritten as a sum over a series of harmonics Q_{kl}, each labeled by a (k,l) pair

$$J_x(t) \;=\; J_{x0} \;+\; \mathrm{Im} \sum_{kl} D_{xkl}\; e^{i2\pi Q_{kl}\, t} \qquad (62)$$

where the horizontal *action harmonic coefficients* are given by

$$D_{xkl}(J_{x0}, J_{y0}) \;=\; \frac{-k}{2\sin[\pi Q_{kl}]} \sum_{ij} V_{ijkl}\; J_{x0}^{i/2} J_{y0}^{j/2}\; e^{i\phi_{0ijkl}} \qquad (63)$$

Similar expressions hold for D_{ykl}, the vertical coefficients. Action harmonic coefficients are readily derived from a single data set – a pair of horizontal and vertical time series – by performing two Discrete Fourier Transforms.

Each action harmonic coefficient is a binomial vector sum over i and j that depends explicitly on the particular values of J_{x0} and J_{y0} used in acquiring the data. For example, if the vertical AC dipole is turned off then $J_{y0} = 0$, so that only V_{ijkl} terms with $j = 0$ continue to contribute. If multiple data sets are taken on a grid of (J_{x0}, J_{y0}) values, and are Fourier analyzed to produce a mesh of coefficients D_{xkl} and D_{ykl}, then it is possible to recover a complete set of individual Hamiltonian coefficients – V_{ijkl} and ϕ_{0ijkl} values.

4.4 A simple numerical example - part 3

Depending on the interpretation of the four quantities Q_X, Q_Y, J_{x0} and J_{y0} in Eqn. 56, this formalism can apply to turn–by–turn data generated by a single particle simulation with no AC dipole, or to measurement data generated by a

real coherent beam driven to a large amplitude by an AC dipole. The Discrete Fourier Transform results are expected to be similar, provided that the four quantities Q_X, Q_Y, J_{x0} and J_{y0} are similar. Of course, the four quantities can not be completely identical, since the AC dipole tune Q_D can never be exactly the same as the betatron tune.

Figure 9 compares three Discrete Fourier Transforms of 2048 turns of turn–by–turn data generated by the numerical simulation. In all three cases a single particle is launched with phase space coordinates corresponding to the center of the AC dipole fixed point shown in Fig. 8. In the first case only the detuning octupoles are turned on, corresponding to the top phase space portrait in Fig. 7.

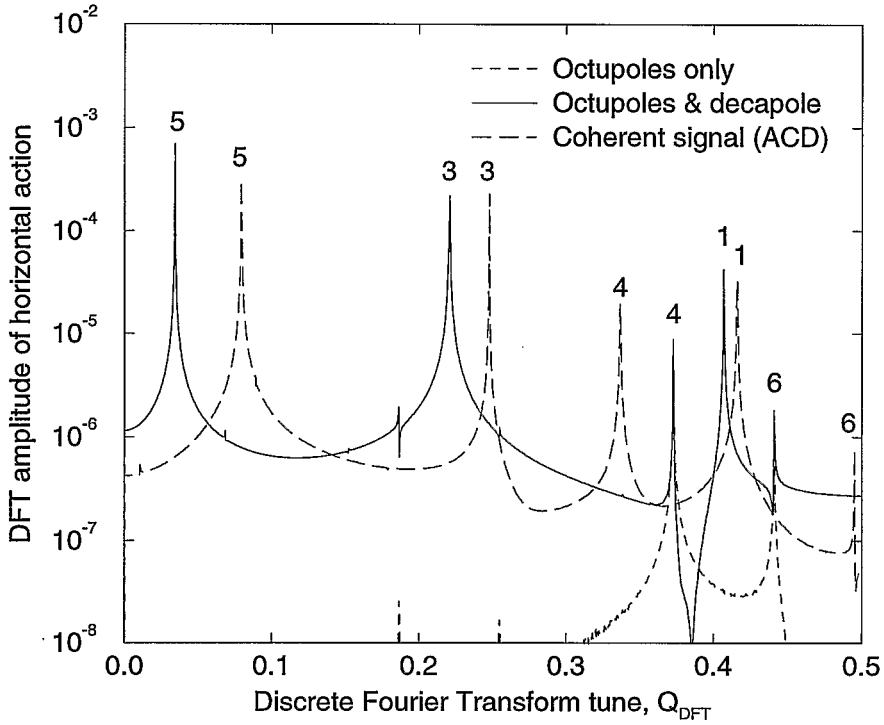

Figure 9: Discrete Fourier Transforms of the horizontal action of a test particle in a numerical simulation. Weak harmonics are seen at $k = 4$ and $k = 6$ when only octupoles are turned on (short dashed line). Strong harmonics at $k = 5$ and $k = 3$ are driven when a decapole is added (solid line). The peaks are shifted when the test particle is launched at the stable fixed point created by turning on an AC dipole at a tune of $Q_D = 59/101 \approx 0.584$ (long dashed line).

Although the octupoles have been arranged to minimize phase space distortions, weak action harmonics are visible at $k = 4$ and $k = 6$. In the second case the decapole is turned on, corresponding to the top portrait in Fig. 8. Much stronger action harmonics are now visible, primarily as expected at $k = 5$, but also at $k = 3$, while the $k = 4$ and $k = 6$ octupole resonances are still visible. The free tune is $Q_X = 0.5932$ in both of these cases.

In the third case the AC dipole is turned on at its nominal tune of $Q_D = 59/101 \approx 0.5842$, a distance $\Delta Q = 0.009$ away from the free tune. The locations of the peaks shift accordingly. For example, the aliased value of the $k = 5$ harmonic moves from $Q_{DFT} = 0.0342$ to $Q_{DFT} = 0.0792$, a factor of 2.32 further away from the origin. Equation 63 predicts that the height of the peak will decrease by almost the same factor, if the V_{ijkl} terms are the same in both cases. In fact the height decreases by a factor of 2.27. This preliminarily confirms that results obtained from a coherent beam driven by an AC dipole can be used to directly infer single particle Hamiltonian coefficients.

Harmonic k	single particle alias	coherent (AC dipole) alias
1	0.4068	0.4158
2	0.1863	0.1683
3	0.2205	0.2475
4	0.3726	0.3366
5	0.0342	0.0792
6	0.4410	0.4950

Table 1: Aliased harmonics visible in the Discrete Fourier Transforms of a single particle and of a simulated coherent signal driven by an AC dipole. The unaliased single particle tune is $Q_X = 0.5932$, and the unaliased AC dipole tune is $Q_D = 59/101 \approx 0.5842$.

4.5 Smear

The number of V_{ijkl} terms is many, and amplitudes $a_x = \sqrt{2\beta_x J_x}$ are often more appealing than actions. Sometimes it is convenient to summarize the turn–by–turn data by three *smear* statistics, which are the standard deviations of the amplitudes, scaled to become dimensionless [2]. The horizontal smear s_{xx} is

given by

$$s_{xx}^2 \equiv \frac{\langle a_x a_x \rangle}{\langle a_x \rangle \langle a_x \rangle} - 1 \tag{64}$$
$$= \sum_{ijkl} \frac{k^2 \, V_{ijkl}^2}{2^{i+j+3} \sin^2[\pi \nu_{kl}]} a_{x0}^{2i-4} a_{y0}^{2j}$$

the vertical smear by

$$s_{yy}^2 \equiv \frac{\langle a_y a_y \rangle}{\langle a_y \rangle \langle a_y \rangle} - 1 \tag{65}$$
$$= \sum_{ijkl} \frac{l^2 \, V_{ijkl}^2}{2^{i+j+3} \sin^2[\pi \nu_{kl}]} a_{x0}^{2i} a_{y0}^{2j-4}$$

and the correlation smear by

$$s_{xy}^2 \equiv \frac{\langle a_x a_y \rangle}{\langle a_x \rangle \langle a_y \rangle} - 1 \tag{66}$$
$$= \sum_{ijkl} \frac{kl \, V_{ijkl}^2}{2^{i+j+3} \sin^2[\pi \nu_{kl}]} a_{x0}^{2i-2} a_{y0}^{2j-2}$$

where it is assumed that $\beta_x = \beta_y = 1$. There is excellent agreement between predicted and measured smears in controlled experiments with a small number of dominant nonlinearities [3, 4].

5 Summary and Conclusions

AC dipoles are potentially very useful in diagnosing nonlinear motion in storage rings like RHIC. The *strong adiabatic drive* method is much preferred if strong enough AC dipoles are available, because it generates clean coherent signals that do not decohere. It is also a non-destructive method which does not lead to emittance growth, and which therefore enables a rapid operational loop of beam based measurement and correction. Horizontal and vertical AC dipoles will be installed in a region of RHIC that is common to both Blue and Yellow rings.

If necessary – if strong enough AC dipoles are *not* available – then a hybrid method using a one turn kicker with a weak AC dipole is also viable. This has the disadvantage of being a destructive technique that leads to filamentation and emittance growth, requiring beam to be re-injected before another measurement, or before attaining reasonable collision conditions. However, it is a null measurement technique that is robust in the presence of rapid decoherence.

If the Hamiltonian coefficients can be measured using AC dipoles, then they can also be reduced by the judicious use of nonlinear correctors. In RHIC many

layers of nonlinear correctors are located in the interaction triplet quadrupoles on either side of every interaction point. The diagnostic situation is then analogous to the measurement and correction of closed orbits – it is not known *prima facie* where the errors come from, but their effects can be measured, and the expected performance of the available correctors can be confirmed.

6 Acknowledgments

We are very grateful for the help and support that Mei Bai, Rhianna Bianco, Wolfram Fischer, and Todd Satogata provided in the preparation of this report.

References

[1] A. Chao et al, PRL 61 (1987) 2752; T. Chen et al, PRL 68 (1992) 33

[2] S. Peggs, Proc. 2nd ICFA workshop, CERN 88-04, and SSC-175 (1988)

[3] N. Merminga, A study of nonlinear dynamics in the Fermilab Tevatron, Ph.D. Thesis, U. Michigan (1989)

[4] M.Y. Li, A study of nonlinear motions in large synchrotrons, Ph.D. Thesis, U. Houston (1990)

[5] S.Y. Lee et al, PRL 67 (1991) 3768; D.D. Caussyn et al, PRA 46 (1992) 7942

[6] T. Satogata et al, PRL 68 (1992) 1838

[7] T. Satogata, Nonlinear resonance islands and modulational effects in a proton synchrotron, Ph.D. Thesis, Northwestern U. (1993)

[8] W. Fischer, An experimental study on the long-term stability of particle motion in hadron storage rings, Dissertation, U. Hamburg (1995)

[9] W. Fischer et al, PRE 55 (1997) 3507

[10] M. Bai et al, PRE 56 (1997) 6002

[11] M. Bai, Overcoming intrinsic spin resonances by the use of an RF dipole, Ph.D. Thesis, U. Indiana (1999)

[12] P. Castro-Garcia, Luminosity and beta function measurements at the electron-positron collider ring LEP, Doctoral Thesis, U. de Valencia (1996)

[13] R. Bianco, T. Satogata,
http://www.rhichome.bnl.gov/AP/Java/acdodo.html